Original Research

Expressional difference, distributions of TGF-β1 in TGF-β1 knock down transgenic mouse, and its possible roles in injured spinal cord

Yan-Bin XiYang[1], Bing-Tuan Lu[1,*], Ya-Zhao[1], Yuan-Zhang[1], Qin-Jie Xia[2], Yu Zou[2], Wei Zhang[3], Xiong-Zhi Quan[3], Su Liu[1,3,4], John W McDonald[3,4], Lian-Feng Zhang[5,*] and Ting-Hua Wang[1,2]

[1]Institute of Neuroscience, Kunming Medical University, Kunming 650500, China; [2]Institute of Neurological Disease, Translational Neuroscience Center, West China Hospital, Sichuan University, Chengdu 610041, China; [3]International Center for Spinal Cord Injury, Hugo W. Moser Research Institute at Kennedy Krieger, Baltimore, MD, 21205, USA; [4]Johns Hopkins University School of Medicine, Department of Neurology and Department of Physical Medicine and Rehabilitation, Baltimore, MD, USA; [5]Key Laboratory of Human Diseases Comparative Medicine, Ministry of Health; Institute of Laboratory Animal Science, Chinese Academy of Medical Sciences(CAMS) & Comparative Medicine Centre, Peking Union Medical College (PUMC), Beijing 100021, China

*These authors contribution is same as first author.

Corresponding authors: Ting-Hua Wang. Emails: tinghua_neuron@263.net and Lian-Feng Zhang. Email: lianfeng_zhang3@yahoo.com.cn

Abstract

Transforming growth factor β1 (TGF-β1) is a multi-functional cytokine implicated in many aspects of mammalian wound healing and scar tissue formation. However, few experiments have so far addressed the potential biological effects of TGF-β1 in the nervous system after injury, in addition to the immune system. In the present study, expressional silencing TGF-β1 was achieved by selecting predesigning hairpins targeting mouse TGF-β1 genes. Four homozygous transgenic offspring were generated and designed as Founder 90, Founder 12, Founder 41 and Founder 46. The down-regulated rates of TGF-β1 in different transgenic mice were also determined. To investigate the potential roles of TGF-β1, we observed changes in the neurological behavior of TGF-β1-knockdown (TGF-β1-kd) mice after spinal cord transection (SCT). Moreover, mRNA levels of inflammatory cytokines, including IL-1, IL-6, IL-10, NF-κB and TNF, were also detected in nucleate cells from blood by real-time PCR. Consequently, different TGF-β1 expressions were detected in multiple tissues, and protein levels of TGF-β1 decreased at different rates relative to that of wild type (WT) ones. The levels of TGF-β1 proteins in TGF-β1-kd mice decreased at most by 57% in Founder 90, which showed a significant recovery in Basso, Beattie, Bresnahan (BBB) scores after SCT compared with that of WT. However, expressions of immune relative genes showed no dramatic difference compared with WT ones. This study is the first to generate TGF-β1 down regulated mice and determine the possible roles of TGF-β1 *in vivo* in different conditions.

Keywords: TGF-β1, knockdown, transgenic mouse, protein expression, distribution and localization, phenotype

***Experimental Biology and Medicine* 2014; 239: 320–329. DOI: 10.1177/1535370213509562**

Introduction

Transforming growth factor, beta (TGF-βs), as family members of NTFs, promote cell survival or induce apoptosis, stimulate cell proliferation or induce differentiation, and their immune functions are mostly anti-inflammatory.[1] It is known that TGF-β1 and -β2 induce, while TGF-β3 seems to inhibit cutaneous scarring.[2] Furthermore, the biological effects of TGF-βs are transduced through the type I (RI) and type II (RII) transmembrane receptors. *In vitro*, TGF-β1 is a potent astrocytic chemotactic agent, causing astrocyte hypertrophy and up-regulation of laminin, fibronectin, and collagen type I synthesis.[3,4] Previous work showed that TGF-β1 protein injection into the subarachnoid space of rats with SCI induced partial restorations in hindlimb motor function.[5] It is, therefore, suggested TGF-β1 may be involved in neuroplasticity following spinal cord injury (SCI). However, the role of intrinsic TGF-β1 is yet to be known. In addition, the relation between TGF-β1 and immune system is also awaiting discovery.

In the present study, we developed a transgenic (Tg) mice line with TGF-β1 knock down by genetic manipulation.

Polymerase chain reaction (PCR) was performed to identify the genotypes of mice. Then, western blot and immunohistochemistry (IHC) were employed to detect the protein expressional levels and localizations of TGF-β1 in multiple tissues of different genotypes Tg mice. These tissues were olfactory bulb, cortex, frontal lobe, basal forebrain, cerebellum, hypothalamus, medulla oblongata, spinal cord, trachea, lung, heart, liver, spleen, kidney, adrenal gland, intestines, skeletal muscles, and epidermis. After the rates of TGF-β1 down-regulation in multiple tissues of different genotypes were evaluated, one of the Founder lines was chosen as the target line because it had the highest value. Then peripheral blood was obtained from the target lines to harvest the nucleate cells so as to explore the expressional level of IL-1, IL-6, IL-10, NF-κB, and TNF by real-time PCR (RT-PCR) in TGF-β1-kd mice. Furthermore, the target lines were also subjected to spinal cord transection (SCT) to observe behavior changes on locomotor functions in hindlimbs after cord transection.

Materials and methods

Animal generation

Animal use and care were in accordance with the animal care guidelines, which conformed to the Guide for the Care and Use of Laboratory Animals published by the US National Institutes of Health (NIH Publication No. 85-23, revised 1996). Mice were housed with free access to food and water and exposed to a 12-h light/dark cycle.

TGF-β1 knock down (TGF-β1-kd) Tg mice with C57BL/6J genetic background were produced by our collaborators in the Institute of Laboratory Animal Science (Chinese Academy of Medical Sciences & Comparative Medicine Centre, Peking Union Medical College, Beijing, China). The generation of the transgenic mice is described as follows. Briefly, at least three silence expression sites of TGF-β1 were designed by software supplied by Invitrogen Company. Then, we selected predesigned short hairpin RNA (shRNAs) targeting the mouse TGF-β1 gene (Mus musculus, Gene ID: 21803) and the reconstruction plasmid for TGF-β1 knock down were designed (Figure 1a) which was also purchased from Invitrogen Company (Beijing, China). The constructed recombinant plasmid was transferred into 293 T cells. The transformants were screened and identified by RT-PCR, semi-quantity PCR and restriction analysis (Figure 1(b) to (d)). The transgene was then isolated from the cloning plasmid and purified by Avr II digestion. Then the mixture was diluted to a final concentration of 5 ng/μL. The final transgenic fragment was microinjected into fertilized mouse eggs (F1 [C57BL/6 × CBA/J] × F1 [C57BL/6 × CBA/J]).

The Tg mice were mated with non-transgenic partners to maintain heterozygozity of the transgene or with transgenic partners to generate homozygous transgenic offspring. In the latter case, transgenic male mice were test mated with two wild-type female mice, and the offspring (15–20 individuals) were analyzed by PCR. Male mice that produced exclusively transgenic offspring were considered homozygous for the transgene. TGF-β1-kd Tg mice and their age-matched, non-transgenic littermates (WT mice) were used.

Real-time PCR

The effects of shRNA targeted to TGF-β1 gene were detected by RT-PCR in transferred 293 T cells, while the expressions of numerous inflammatory cytokines in nucleate cells of peripheral blood (PB) from mice were also estimated. Total 250 μL PB was obtained from tails of both target Tg mice and the WT ones ($n = 6$). The mRNA expressions of multiply genes, including IL-1, IL-6, IL-10, NF-κB, and TNF, were detected by RT-PCR.

Trizol reagent (Invitrogen) was used to isolate total RNA. cDNA was synthesized by using Oligo(dT)^{18} and MMLV reverse transcriptase (Promega, Madison, WI). Multiple genes were detected by RT-PCR. GAPDH was used as a reference and subtracted for net changes. The sequences of primers were recorded in Table. Gene primers were synthesized by Shengon (Shanghai, China) Company. The cDNA was 10-fold serially diluted to seven concentrations for the standard curve.

To analyze the mRNA expressions of TGF-β1 in transformants, RT-PCR protocol was applied using an ABI 5700 instrument (Bio-Rad Laboratories, Shanghai, China). Reactions were performed in a 20 μL volume with 0.25 μM primers, 5 mM $MgCl_2$, nucleotides, Taq DNA polymerase, and buffers were included in the DNA Master SYBR Green I mix (Applied Biosystems, Shanghai, China). Specificity of the amplification products was confirmed by melting curve analysis. PCR was performed by the denaturation step at 95°C for 3 min, followed by 35 cycles at 95°C for 10 s, annealing for 10 s, and at 72°C for 30 s. Fluorescent signals from PCR products were recorded at 85.5°C for 5 s. Gene mRNA levels were normalized as the ratio of the fluorescence intensity from target gene to that of GAPDH.

Semi-quantity PCR

Preparation for RNA samples were described as above. Then the total RNA was eluted in 20 μl RNase-free Water (Gibco Life Technologies, Rockville, MD). The RNA was kept on ice and their concentrations were measured by a Nanodrop spectrophotometer (ND-1000). An equal amount of RNA (4 μg) was used for each experiment. Semi-quantity PCR for the TGF-β1 was performed. The following primers were used: sense, 5′CGGAGCATGGAA GTCACAG 3′; anti-sense, 5′ ACCACAGCCAGGAAACCC 3′. The product length of PCR is 437 bp. Gene primers were synthesized by TaKaRa Company.

Experiments were duplicated to verify the results. For RNA amplification, the first-strand cDNA was synthesized from 4 μg of total RNA, using Revert AidTM First Strand cDNA Synthesis Kit (Fermentas Company, USA). PCR was then carried out using the PCR Master Mix Kit (Fermentas Company, USA) for 35 cycles, consisting of denaturation at 94°C for 1 min, annealing for 1 min, and extension at 72°C for 1 min. Then PCR products were electrophoresed in 1% agarose gel stained with ethidium bromide and visualized using an ultraviolet gel imager (BIO-GEL, BIP-RAD). The image analysis was performed by SYN Gene Tool (LIVE Science, Bio-Rad, Alfred, CA).

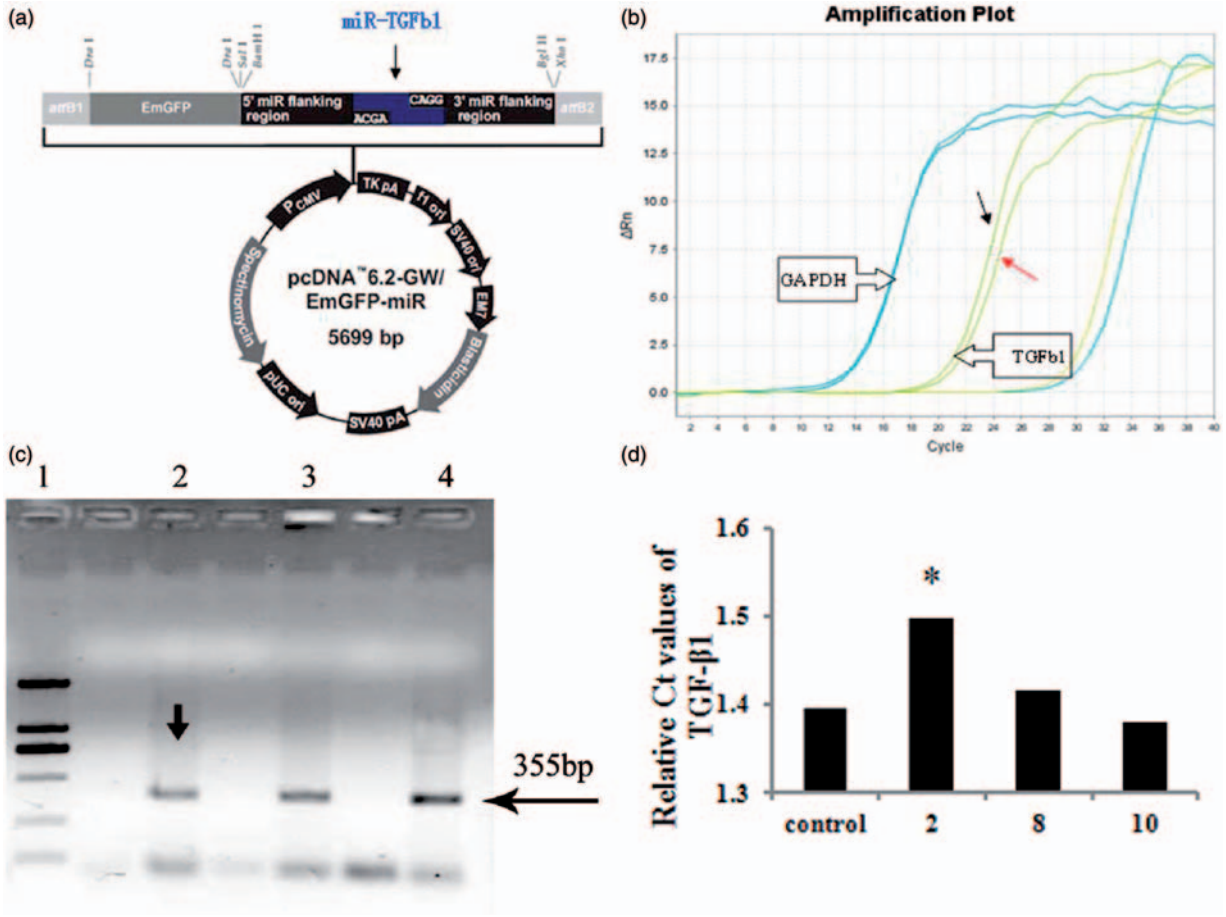

Figure 1 Recombination plasmid for Tg mice with TGF-β1 knock down. (a) This shows the schedules of recombination plasmid for pcDNA6.2-GW/ EmGFP-miR of TGF-β1 gene silence, which composed with 5699 nucleotides. The 293 T cells were transfected with the transgenic vectors (pcDNA3.1 (+) of pcDNA6.2-GW/ EmGFP-miR-TGF-β1). RT-PCR was employed to evaluate the effects of PDGF-BB down-regulation transformants. (b) This shows the amplification plot of RT-PCR. Red arrows show the selected cell lines as they had the lowest levels. Black arrow indicates the control ones. (c) This shows the represented bands of semi-quantity PCR products electrophoresed in 1% agarose gel stained with EB. Lane 1: DL2000 DNA Marker (from up to down: 2000 bp, 1000 bp, 750 bp, 500 bp, 250 bp, 100 bp, respectively); Lane 2: negative control; Lane 3: positive control; Lane 2–4: 293 T cells transfected with silence expression vector for TGF-β1 gene (from lane 2 to 4: No. 2, No. 8, and No. 10, respectively). Panel (d) reveals the relative Ct values for TGF-β1 levels in transfected 293 T cells. Arrows in (c) and ''*'' in (d) indicate the target transformants for TGF-β1 expressional knock down was No. 2

Assessment of genotypes

The inserted fragment was identified by PCR. For TGF-β1-kd lines, the following primers were used: sense, 5′ GAGCAAAGACCCCAACGAG 3′; antisense, 5′ TTATGAACAAACGACCCAAC C 3′. The length of PCR product is 419 bp. Briefly, genomic DNA from mice tail were isolated and purified for PCR analysis. PCR was carried out using the PCR Master Mix Kit (Fermentas Company, Glen Burnie, Maryland, USA) for 35 cycles, consisting of denaturation at 94°C for 30 s, annealing at 60°C for 30 s, and extension at 72°C for 30 s. Then RT-PCR products were electrophoresed in 1% agarose gel stained with ethidium bromide and visualized using an ultraviolet gel imager (BIO-GEL, BIP-RAD). The image analysis was performed by SYN Gene Tool (LIVE Science, USA).

Expressions of TGF-β1 protein in different TG mouse

To investigate the level of TGF-β1 protein, multiple tissues described above were obtained from mice with different genic genotypes. After carefully rinsing in cooled PBS, the hippocampus of each was homogenized on ice in a Lysis Buffer containing 0.05 M Tris–HCl (pH 7.4, Amresco), 0.5 M EDTA (Amresco), 30% TritonX-100 (Amresco), NaCl (Amresco), 10% SDS (Sigma), and 1 mM PMSF (Amresco), and centrifuged at 12,000 rpm for 30 min. The supernatant was then obtained and stored at −80°C for later use. Protein concentration was assayed with BCA reagent (Sigma, St. Louis, MO, USA). A 20 µl aliquot of the samples was loaded on to each lane and electrophoresed on 12% SDS-polyacrylamide gel (SDS-PAGE) for 2.5 h at a constant voltage of 120 V. Proteins were transferred from the gel to a nitrocellulose membrane for 6.5 h at 24 V. The membrane was blocked with phosphate-buffered saline containing 0.05% tween-20 (PBST) with 10% nonfat dry milk overnight at 4°C for 12 h, and then the membrane was washed three times for 10 min each time. They were then rinsed with PBST and incubated with the primary antibody for TGF-β1 (1:800, Chemican) at 4°C for 24 h. After washing three

times for 10 min each, the membrane was incubated with a HRP-conjugated goat anti-rabbit IgG (1:5,000; Vector Laboratories, CA) for 2 h at room temperature and washed as described earlier. The membrane was developed in ECM kit, and then pictured by Bio-Gel Imagining system equipped with Genius synaptic gene tool software. Densitometry analysis for TGF-β1 protein was performed. β-tubulin (1:500, Santa cruz) was used as internal control.

Immunohistochemistry

After anesthesia with 3.6% chloral hydrate (1 mL/100 g), mice were perfused with 150 mL of cold phosphate-buffered saline (PBS) for 5 min followed by 150 mL of 4% paraformaldehyde solution for 30 min. Multiple tissues including the olfactory bulb, whole brain, spinal cord, skeletal muscles, lung, heart, liver, spleen, kidney, adrenal gland, intestines, and epidermis from Tg mice were harvested. They were post-fixed for 6–12 h and then immersed in 0.1 M PBS containing 20% sucrose overnight till the specimen sank to the bottom of the bottle. Sections of 20 μm thickness were cut in a freezing microtome (Leica CM1900, Germany), collected in a plate of 24 wells, rinsed with 0.01 M PBS three times, each for 5 min, and then soaked in PBS containing 3% H_2O_2 for 30 min at room temperature to block the endogenous peroxidase activity. After immersing in 0.01 M PBS containing 5% goat serum and 0.3% TritonX-100 solution at 37°C for 30 min, they were subsequently incubated at 4°C overnight with 2% goat serum containing goat polyclonal antibodies TGF-β1 (1:800, Santa Cruz). They were washed three times (5 min each time) in 0.01 M PBS containing 0.1% Tween-20 (PBST), and incubated in reagents I and II from the PV-9000 Reagent Kit (Chemicon, Anti-Rabbit/Mouse Poly-HRP IHC Detection Kit, USA), each for 30 min at 37°C. It was again rinsed five times, each for 5 min in 0.01 M PBST. Finally, the sections were detected by DAB staining. Negative control was performed by replacing the primary antibody with 2% goat serum to ascertain the specificity of antibody staining. Immunoreactive products were observed and photographed with a light microscope (Leica. DMIRB, Germany) coupled with a computer-assisted video camera.

Surgical procedures

For surgical operation, the mice were anaesthetized with intraperitoneal injection of 3.6% chloral hydrate (1 mL/100 g). The spinal cord was exposed at vertebral levels (T9–T11) and the cord transected at the T10 level. In sham-operated mice, the cord was spared. After operation, the mice received daily injections of Benzyl-penicillin (dosage 5 IU) for three days. Manual bladder evacuation was applied three times daily.

Functional evaluations

Hindlimb locomotor function of the mice was assessed using the Basso, Beattie, Bresnahan (BBB) score[6] at 1, 3, 10, and 17 days post-operation (dpo). The BBB scores after transection ranged from 0 to 21. Animals were allowed to walk around freely in an open-field for 4 min while movements of hindlimbs were closely observed. According to the scoring system, rank includes the frequency and quality of hindlimb movements. Three persons in a double blind situation conducted the evaluations. The average of the three scores by the three observers was calculated. All behavioral evaluations were performed daily at 8:00 to 9:00. Before testing, bladders were evacuated, as spontaneous bladder contraction often accompanied hind limb activity.

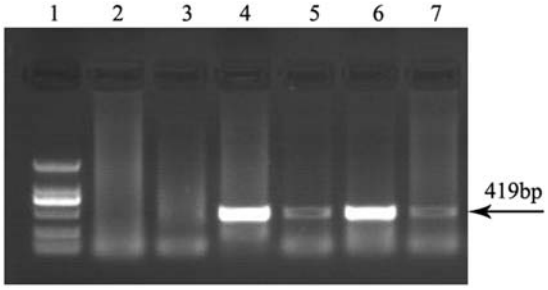

Figure 2 Genotypes detection for the TGF-β1-kd Tg mice. The positive Tg mice detected by PCR. This figure shows the representative lanes of products electrophoresed in 1% agarose gel stained with EB. Lane 1: DNA Marker DL 2000 (from up to down: 2000 bp, 1000 bp, 750 bp, 500 bp, 250 bp, and 100 bp respectively). Lanes 2–7: The PCR productions of inserted fragment from different heterozygous transgenic offspring of TGF-β1-kd lines. Lanes 2 and 3: WT; Lane 4: Founder 90; Lane 5: Founder 12; Lane 6: Founder 41; and Lane 7: Founder 46

Results

Genotypes detection

Five heterozygosis transgenic offspring of TGF-β1-kd lines were obtained. Four of them could generate offspring, which were designated as Founder 90, Founder 12, Founder 41, and Founder 46. The Tg mice with inserted fragment, identified by PCR, were regarded as positive ones (Figure 2).

Protein expressional changes of TGF-β1 in multiple tissues of TG with different genotypes

Results of Western blot, which was performed on multiple tissues of four genotypes TG (Founder 90, Founder 12, Founder 41, and Founder 46), indicated that TGF-β1 expressions were down-regulated by different percentages in the four kinds of TG (Figures 3 and 4). The down-regulated rates of protein were calculated as follows: O.D.(WT – Founder)/O.D. WT × 100% (O.D. means optical density). Founder 90 was chosen as the target lines as it had the highest value.

Distributions of TGF-β1 in multiple tissues

Immunoreactivity (IR) of TGF-β1 was detected in all tissues explored in this experiment. The negative controls did not exhibit any specific immune-staining in the intestines (Figure 5s) nor the spinal cord (Figure 5t).

Olfactory bulb

Immunoreactions of TGF-β1 was seen in basal cells, supporting cells, neurons, apical cytoplasmic region of

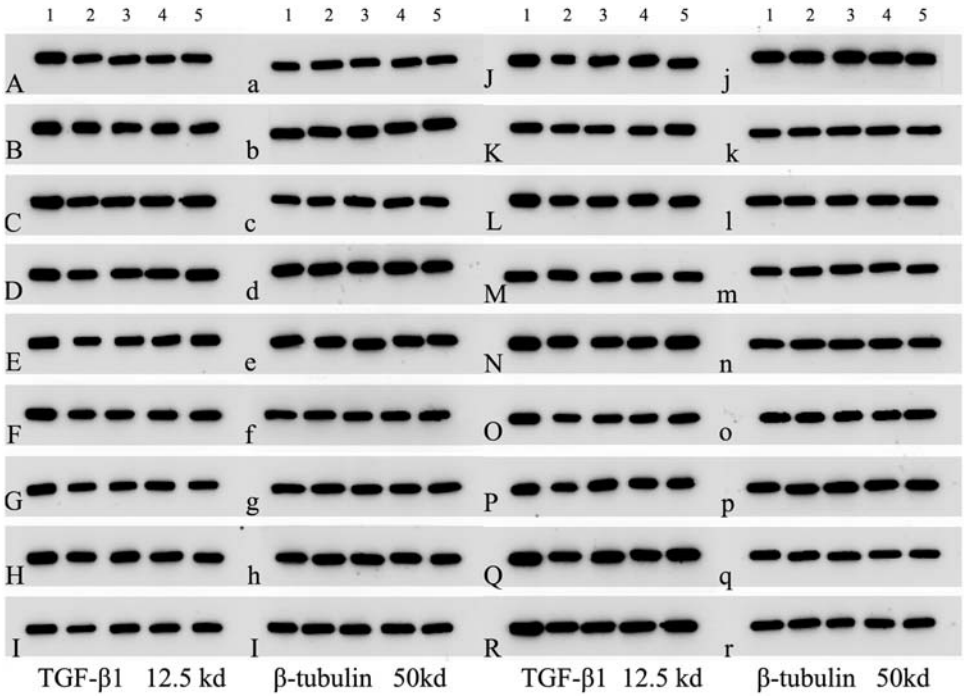

Figure 3 Protein expressions of TGF-β1 detected by WB in different tissues. Lanes 1–7, TGF-β1 protein expression; Lane 1, WT; Lane 2: Founder 90; Lane 3: Founder 12; Lane 4: Founder 41; Lane 5: Founder 46. A, a: olfactory bulb; B, b: cortex; C, c: frontal lobe; D, d: basal forebrain; E, e: cerebellum; F, f: hypothalamus; G, g: medulla oblongata; H, h: spinal cord; I, i: trachea; J, j: lung; K, k: heart; L, l: liver; M, m: spleen; N, n: kidney; O, o: adrenal gland; P, p: intestines; Q, q: skeletal muscles; R, r: epidermis. Beta-tubulin was chased as the control

olfactory epithelium, lamina propria, and gland's cell cytoplasm. The positive reactions were seen in a majority of the cytoplasm (Figure 5a).

Brain

The distributions of TGF-β1 immuno-positive neurons and glias were observed within the cortex, basal brain, frontal lobe, cerebellum, hypothalamus, and medulla oblongata. They occurred in all layers of the cortical regions examined in this study, including the external pyramidal and internal pyramidal layers. The somata and proximal dendrites with TGF-β1 IR were also observed in the brain stem, granular cells, and in axon-like fibers in the molecular cell layer. Immunoreaction products of TGF-β1 were mainly observed in the cell bodies, processes, and perikarya of these neurons. Nuclei of these cells were not stained (Figure 5(b) to (d)).

Spinal cord

The TGF-β1 immuno-positive profiles were present in neurons of the dorsal horn, ventral horn as well as white matter of the spinal cord. The IR could be seen in the cytoplasm and processes, but not in the nucleus (Figure 5(e) to (g)).

Lung

The TGF-β1IR was found in the epithelial cells, vascular endothelial cell, as well as white blood cell. The IR was seen in the cytoplasm but not in the nuclei (Figure 5i).

Liver

TGF-β1 staining was distributed in hepatocytes, liver acinus, sinusoid as well as vascular endothelial cell. They were mainly seen in the cytoplasm (Figure 5l).

Spleen

IR of TGF-β1 was detected in Tunica media of artery, subendothelial smooth muscle cell, and endotheliocyte. The immunoreactions were seen in the cytoplasm, but not in the nucleus (Figure 5m).

Kidney

Representative IR for TGF-β1 in renal section of Tg mice showed diffuse positive staining within the renal cortex, medullary interstitial cells, as well as the peritubular capillaries (Figure 5(n) and (o)).

Adrenal gland

The majority of TGF-β1 positive cells were located underneath the capsule, in the adrenal cortex with cytoplasm stained (Figure 5p).

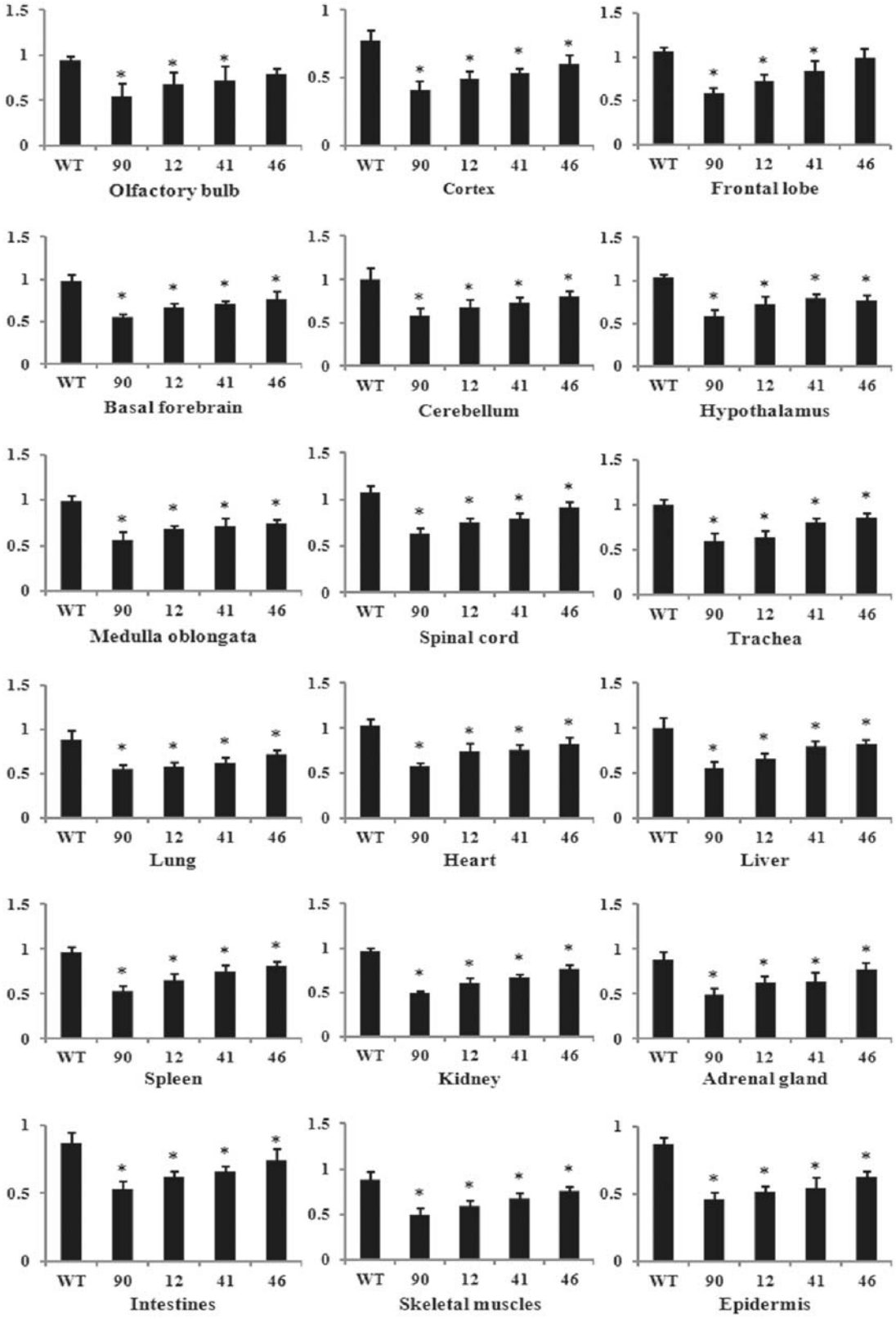

Figure 4 Relative expressions of TGF-β1 in different tissues of Tg mice. It shows the relative optical density (OD) of TGF-β1 protein levels in multiple tissues of Tg mice and that of WT ones ($n = 6$). Values plotted are means ± SD. According to formula of the down-regulated rates of TGF-β1 protein, the average down-regulated rates of the four transgenic lines were calculated and described as follows. The average rates were 57%, 32%, 18%, and 17% in Founder 90, Founder 12, Founder 41, and Founder 46, respectively. The relative expressions of TGF-β1 proteins in Founder 90, Founder 12, and Founder 41 were significantly different compared with that of WT ones ($P < 0.05$). *Compared with WT, $P < 0.05$

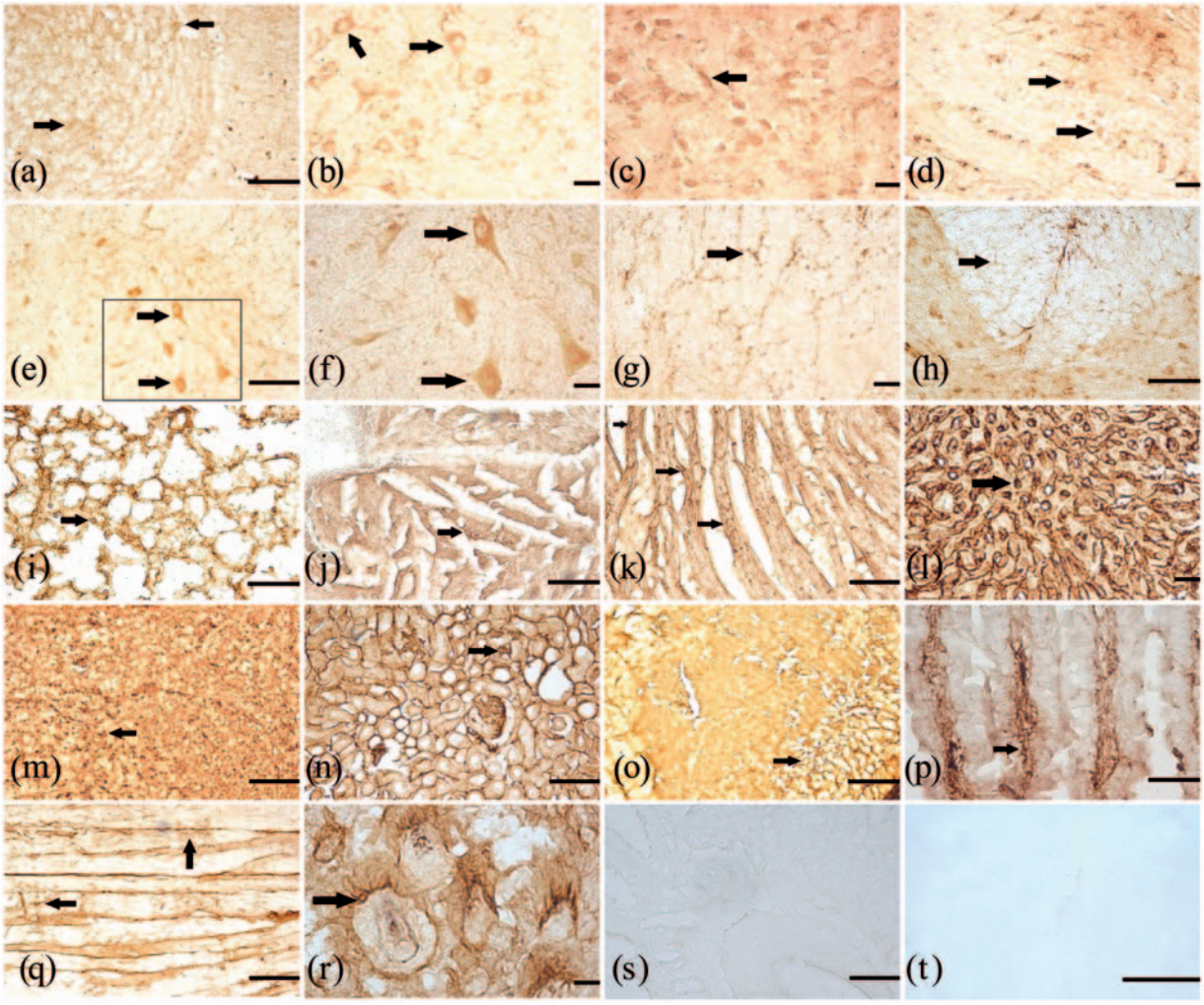

Figure 5 Locations of TGF-β1 in multiply tissues of Tg mice. The arrow shows the representative IR of TGF-β1. (a) olfactory bulb (arrows show the staining neurons); (b) frontal lobe (arrows show the staining neurons); (c) basal forebrain (arrows show the staining neurons); (d) hypothalamus (arrows show the staining neurons); (e–h): spinal cord (arrows show e and f: motor neuron in the ventral horn; g and h: staining fibers in the whiter matter); (i) lung (arrows show epithelial cells); (j and k) heart; (l) liver (arrows show the staining hepatocytes); (m) spleen (arrows show endothelia cells); (n) kidney (arrow show medullary interstitial cells); (o) adrenal gland (arrows show immunostaining in the adrenal cortex); (p) intestines; (q) skeletal muscles (arrows show staining in sarcoplasm); (r) epidermis (arrows show staining basal cells); (s) control of intestines; (t) control of spinal cord. Note: Magnifications: b, c, d, f, g, l and r: 400×; T: 25×; other: 200×; Scale bar: 10 μm. (A color version of this figure is available in the online journal)

Intestine

The immunopositive files of TGF-β1 were dispersed in lamina propria, epithelium mucosae, and muscular layer. The immune-positive staining was primarily in the cytoplasm and partial cytolemma (Figure 5q).

Muscle

The TGF-β1 staining was localized to the sarcolemma in skeletal muscle of mice (Figure 5r). In the sarcoplasm, there was staining in a transverse striation pattern at regular intervals for the length of a sarcomere. Immunostaining for TGF-β1 also showed positive staining in coronary arteries of hearts (Figure 5(j) and (k)).

Epidermis

The positive reactions of TGF-β1 were detected in the epidermis of Tg mice. The IR was found in cytoplasm and cytolemma of basal cells and follicular epithelium (Figure 5s).

Phenotypes analysis in TGF-β1-kd mice

Inflammatory-relative gene expressions

Compared with that of WT mice, the gene levels of IL-1, NF-κB, and TNF showed no significant difference in TGF-β1-kd Tg ones ($P > 0.05$). The mRNA expressions of IL-6 and IL-10 did not reach the detectable level in the PB (Figure 6).

Locomotor functions evaluation

The BBB scores were 0 in all mice subjected to operation at 1 dpo. They increased gradually from 3 to 17 dpo in all the SCT operated mice, but most significantly in the TGF-β1-kd mice (Founder 90). At 3 dpo, the BBB scores in sham-operated mice reached 21 and kept this rank during the following observation. The recovery of motor function in

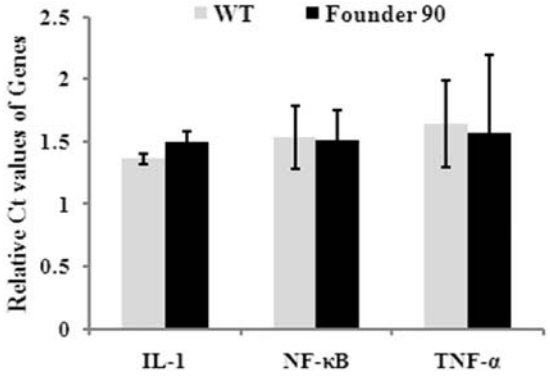

Figure 6 The relative gene expressions of IL-1, NF-κB and TNF in Tg mice. The figure indicates the relative Ct values of IL-1, NF-κB and TNF genes in both of Tg mice and WT ones, which were detected by RT-PCR ($n = 6$). Values plotted are means ± SD

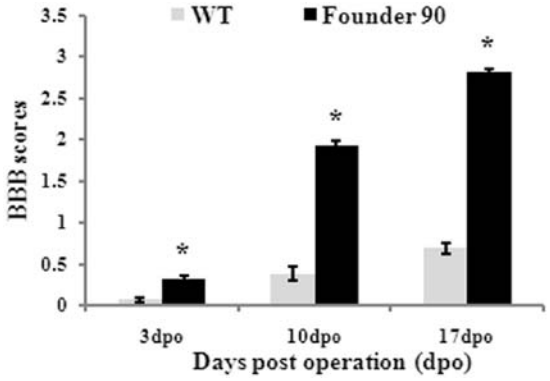

Figure 7 Hindlimb locomotor function evaluation in spinal cord transected Tg mice. The figure shows the BBB scores in both of TGF-β1-kd mice (Founder 90) and WT ones ($n = 6$). The data showed that the BBB scores in sham-operated mice were 21, and 0 in all mice subjected to SCT at 3 dpo. They increased gradually from 3 to 28 dpo in all the operated mice, but most significantly in the TGF-β1-kd mice ($P < 0.05$). Values plotted are means ± SD. *Compared with WT, $P < 0.05$

hindlimbs in TGF-β1-kd mice showed a greater increase, compared with that of WT ones ($P < 0.05$), confirming that TGF-β1 interference exerts a protective effect for the injured spinal cord, which is useful for the recovery of locmotor function (Figure 7).

Discussion

The present study is the first to generate different expressional levels of TGF-β1 transgenic mice, which demonstrated that delivering shRNAs targeting TGF-β1 could induce TGF-β1 expressional decrease in transgene mice, especially in the central nervous system. Also, the expressional decrease in TGF-β1 protein showed variability in different phenotypic transgenic lines. The results detected by Western blot showed that the highest value (nearly 60%) was detected in Founder 90, while the lowest was detected in Founder 46 (17%). In addition, we explored the systemic distribution of TGF-β1 in different tissues of Tg mice, including olfactory bulb, basal forebrain, cerebellum, cortex, hypothalamus, frontal lobe, medulla oblongata, spinal cord, lung, heart, liver, spleen, kidney, adrenal gland, intestines, skeletal muscles, and epidermis. Reduction of TGF-β1 expression by 57% in Founder 90 could induce improvement in hindlimb locomotor, but made no effect on the expressions of various inflammatory-relative genes. Herein, the research (i) created serial new transgenic mice models of TGF-β1 down-regulation; (ii) reported the systematic distributions of TGF-β1 in Tg mice; and (iii) provided information on transgenic phenotypes for further investigations.

Our results of PCR for genotypes detection, which showed that the inserted fragments (419 bp) were detected in four Tg offspring of TGF-β1-kd lines, indicated that new Tg mice model of TGF-β1-kd lines were obtained successfully by genetic manipulation. This study generated four kinds of available Tg mice, which were designated Founder 90, Founder 12, Founder 41, and Founder 46. The result obtained from Western blot analysis also showed that delivering shRNAs for TGF-β1 effectively induced a TGF-β1 expressional decrease in Tg mice.

RNA interference (RNAi) is an extremely effective tool for studying gene function in almost all metazoan and eukaryotic model systems. RNAi in mice, through the expression of short hairpin RNAs (shRNAs), offers something not easily achieved with traditional genetic approaches-inducible and reversible gene silencing.[7,8] The present results show that delivering shRNAs-TGF-β1 can induce TGF-β1 expressional reduction in mice. Random integration of transgenic fragment effectively reduced the systemic expressions of TGF-β1 in Tg mice. However, the expressed decrease in TGF-β1 protein showed variability in different phenotypic lines, indicating that the highest rates of TGF-β1 down-expression (57%) were detected in Founder 90, while that of Founder 46 only decreased by 17%. The diverse expressional changes of TGF-β1 protein in four kinds of Tg mice might have resulted because of the different inserted sites used for the recombination vectors in the target gene.

Furthermore, some unknown mechanisms of post-transcription regulation in different tissues might induce the different levels of TGF-β1 expressions in multiple tissues. TGF-β1 is extensively post-transcriptionally regulated, and reports previously demonstrated specific activation of TGF-β1 translation in response to stimuli including glucose, platelet-derived growth factor, TGF-β1 itself,[9,10,11] and so on. Recently, research has shown that miRs also target TGF-β1 directly, further emphasizing the important role that miRs play in TGF-β1-directed cellular responses, and demonstrating a novel mechanism by which TGF-β1 synthesis may be controlled.[12]

Additionally, the survey of TGF-β1 distributions was made in Tg mice by IHC detection, which revealed the morphological information of TGF-β1 in detail.

In summary, this study provided Tg mice lines with TGF-β1 down-regulation and the systemic morphologic information for further research. Our results showed that TGF-β1 proteins were widespread in multiple tissues, especially in nervous systems, intestines, and epidermis. These results indicated that TGF-β1 might play multiply different

biologic roles according to the different cell types. Moreover, the present study generated four genotypes TGF-β1 Tg mice of expressional down-regulated by different folds, which supplied multiple genotypes Tg mice sources for further research by others.

Since 1980s, TGF-β has emerged as a family of growth factors involved in essential embryological and physiological processes. The three TGF-β isoforms described in mammals (TGF-β1, TGF-β2, TGF-β3) have prominent functions related to morphogenetic events, epithelial–mesenchymal interactions, and differentiation.[13,14] In normal adult animals, TGF-βs (1–3) are ubiquitously and abundantly expressed in neurons and glia cells in both CNS and PNS.[15–17] Furthermore, knockout mice have revealed their importance in regulating inflammation and tissue repair.[18,19] It is expected that the up-regulation of TGF-β1 would be beneficial to the survival and repair of injured motoneurons and contribute to neuroplasticity in the injured cord during the critical stage of synaptic reorganization.[20]

The data showed that TGF-β1-kd promotes partial functional improvement in hindlimbs of Tg mice after SCI. This indicates that there may be an association between the endogenous expression of TGF-β1 and the maintenance of motor neuron activity. During the acute phase of SCI, the formation of inhibitory molecules and extracellular matrix, such as IL-6, TGF-α, and TGF-β, would lead to the proliferation and hypertrophy of the astrocytes forming a scar that blocks the passage of axonal outgrowths.[3,4,21–23] Given this fact, we postulate that the functional improvement seen in TGF-β1-kd Tg mice may be dependent on the interference with astrocyte hypertrophy and scar formation induced by TGF-β1.

In the immune system, TGF-β1 down-regulation had no effect on the expression of some inflammation relative genes, such as IL-1, NF-κB, and TNF. It is suggested that (i) reduction TGF-β1 expressions by 57% in Tg mice might have no interference with its activity in regulating inflammation and anti-inflammation or (ii) the importance performance in inflammatory response and tissue repair of TGF-β1 might be triggered by suitable stimulus but not expressional reduction. Otherwise, the gene expressions of IL-6 and IL-10 were not detected in the PB of mice in the present research. We postulate that the mRNA levels of IL-6 and IL-10 genes in PB of mice were too limited and below the minimum level for experimental detection.

In conclusion, the present study established new transgenic mice lines with extensive down-regulation of TGF-β1. We also supplied (i) the down-regulated rates and systemic distributions of TGF-β1 protein in four phenotypic transgenic mice, which provide pieces of promise information for further investigation by using these transgenic phenotypes and (ii) evidence which demonstrated that TGF-β1 play an important role in motor neuroplasticity following SCI.

Author contributions: All authors participated in the design, interpretation of the studies and analysis of the data and review of the manuscript. THW, LFZ, YBX, BTL, YZ and YZ conducted the experiments. BTL, YZ, YZ, QJX, YZ, WZ, and XZQ supplied critical animals, and YBX wrote the manuscript. SL and MWJ were in charge of English writing.

ACKNOWLEDGEMENTS

This work is supported by National Natural Science Foundation of China (Grant No. 81100911) and Key Project of the Applied Basic Research Programs of Yunnan Province in China (Grant No. 2012F001).

REFERENCES

1. Bottner M, Krieglstein K, Unsicker K. The transforming growth factor-betas: structure, signaling, and roles in nervous system development and functions. *J Neurochem* 2000;**75**:2227–40
2. Shah M, Foreman DM, Ferguson MW. Neutralisation of TGF-beta 1 and TGF-beta 2 or exogenous addition of TGF-beta 3 to cutaneous rat wounds reduces scarring. *J Cell Sci* 1995;**108**:985–1002
3. Toru-Delbauffe D, Baghdassarian D, Both D, Bernard R, Rouget P, Pierre M. Effects of TGF beta 1 on the proliferation and differentiation of an immortalized astrocyte cell line: relationship with extracellular matrix. *Exp Cell Res* 1992;**202**:316–25
4. Gagelin C, Pierre M, Gavaret JM, Toru-Delbauffe D. Rapid TGF beta 1 effects on actin cytoskeleton of astrocytes: comparison with other factors and implications for cell motility. *Glia* 1995;**13**:283–93
5. Hamada Y, Ikata T, Katoh S, Katoh K, Niwa M, Tsutsumishita Y, Fukuzawa K. Effects of exogenous transforming growth factor-beta 1 on spinal cord injury in rats. *Neurosci Lett* 1996;**203**:97–100
6. Basso DM, Beattie MS, Bresnahan JC. A sensitive and reliable locomotor rating scale for open field testing in rats. *J Neurotrauma* 1995;**12**:1–21
7. Bernstein E, Denli AM, Hannon GJ. The rest is silence. *RNA* 2001;**7**:1509–21
8. Holen T, Amarzguioui M, Wiiger MT, Babaie E, Prydz H. Positional effects of short interfering RNAs targeting the human coagulation trigger tissue factor. *Nucleic Acids Res* 2002;**30**:1757–66
9. Fraser D, Wakefield L, Phillips A. Independent regulation of transforming growth factor-beta1 transcription and translation by glucose and platelet-derived growth factor. *Am J Pathol* 2002;**161**: 1039–49
10. Fraser D, Brunskill N, Ito T, Phillips A. Long-term exposure of proximal tubular epithelial cells to glucose induces transforming growth factor-beta 1 synthesis via an autocrine PDGF loop. *Am J Pathol* 2003;**163**: 2565–74
11. Zhang M, Fraser D, Phillips A. ERK, p38, and Smad signaling pathways differentially regulate transforming growth factor-beta1 autoinduction in proximal tubular epithelial cells. *Am J Pathol* 2006;**169**: 1282–93
12. Martin J, Jenkins RH, Bennagi R, Krupa A, Phillips AO, Bowen T, Fraser DJ. Post-transcriptional regulation of transforming growth factor Beta-1 by microRNA-744. *PLoS One* 2011;**6**:e25044
13. Dünker N, Krieglstein K. Targeted mutations of transforming growth factor-beta genes reveal important roles in mouse development and adult homeostasis. *Eur J Biochem* 2000;**267**:6982–8
14. Goumans MJ, Mummery C. Functional analysis of the TGFbeta receptor/Smad pathway through gene ablation in mice. *Int J Dev Biol* 2000;**44**:253–65
15. Flanders KC, Ren RF, Lippa CF. Transforming growth factor-betas in neurodegenerative disease. *Prog Neurobiol* 1998;**54**:71–85
16. Lippa CF, Smith TW, Flanders KC. Transforming growth factor-beta: neuronal and glial expression in CNS degenerative diseases. *Neurodegeneration* 1995;**4**:425–32
17. Peress NS, Perillo E. Differential expression of TGF-beta 1, 2 and 3 isotypes in Alzheimer's disease: a comparative immunohistochemical study with cerebral infarction, aged human and mouse control brains. *J Neuropathol Exp Neurol* 1995;**54**:802–11
18. Shull MM, Ormsby I, Kier AB, Pawlowski S, Diebold RJ, Yin M, Allen R, Sidman C, Proetzel G, Calvin D, Annunziata N, Doetschman T.

Targeted disruption of the mouse transforming growth factor-beta 1 gene results in multifocal inflammatory disease. *Nature* 1992;**359**:693–9
19. Kulkarni AB, Huh CG, Becker D, Geiser A, Lyght M, Flanders KC, Roberts AB, Sporn MB, Ward JM, Karlsson S. Transforming growth factor beta 1 null mutation in mice causes excessive inflammatory response and early death. *Proc Natl Acad Sci USA* 1993;**90**:770–4
20. Li F, Wang L, Jin XM, Yan CH, Jiang S, Shen XM. The immunologic effect of TGF-beta1 chitosan nanoparticle plasmids on ovalbumin-induced allergic BALB/c mice. *Immunobiology* 2009;**214**:87–99
21. Logan A, Green J, Hunter A, Jackson R, Berry M. Inhibition of glial scarring in the injured rat brain by a recombinant human monoclonal antibody to transforming growth factor-beta2. *Eur J Neurosci* 1999;**11**:2367–74
22. Raivich G, Jones LL, Werner A, Blüthmann H, Doetschmann T, Kreutzberg GW. Molecular signals for glial activation: pro- and anti-inflammatory cytokines in the injured brain. *Acta Neurochir Suppl* 1999;**73**:21–30
23. Rabchevsky AG, Weinitz JM, Coulpier M, Fages C, Tinel M, Junier MP. A role for transforming growth factor alpha as an inducer of astrogliosis. *J Neurosci* 1998;**18**:10541–52

(Received July 20, 2012, Accepted August 26, 2013)